Simple Model for Swelling-Induced Stresses in a Supported Polymer Thin Film

T. Z. FU,[1] C. J. DURNING,[1]* and H. M. TONG[2]

[1]Department of Chemical Engineering and Applied Chemistry, Columbia University, New York, New York 10027, and [2]IBM Research Division, T. J. Watson Research Center, Yorktown Heights, New York 10598

SYNOPSIS

Solvent transport in multilayer thin film structures can induce damaging stresses. It is important to understand these quantitatively for the design of processing methods for microelectronics manufacture. As a model for such systems, this article focuses on the connection between solvent transport in a thin, supported film and the induced bending curvature of the film/substrate combination. We develop a simple mechanical model to calculate the bending curvature based on the transport-induced stresses. A phenomenological moving boundary description of non-Fickian solvent transport often found in glassy polymers has been used. The evaluation of dimensionless bending curvature for a number of generic cases is presented. As an application of the model, experimental data for a polyimide (PI)/quartz-*n*-methyl-2-pyrrolidinone (NMP) system involving significant swelling (15–20%) of the PI film is analyzed. The analysis shows that the measured bending during the transport of NMP in the PI film compares well with that predicted based on an "intermediate," non-Fickian diffusion mechanism of NMP, consistent with the finding obtained from a laser interferometric study. Estimation of the swelling-induced stress shows that it is large and as significant as that due to thermal "curing."

INTRODUCTION

The success of multilayer packaging technologies in building microelectronic devices relies, in part, on the understanding and proper control of internal residual stresses within the polymer dielectrics. These stresses are generated, for instance, during the removal of the casting solvent and the thermal "curing" of the polymer. They can distort or damage the circuitry, leading to local or catastrophic delamination in the integrated circuit boards. Obviously, the magnitudes of such internal stresses should be minimized to achieve the desired performance and reliability of microelectronic devices.

Several efforts have been reported to understand stress development during heat treatments of polymers.[1-4] Surprisingly, relatively few efforts have been devoted toward the understanding of the effect of the transport of low molecular weight species on the stress development in multilayered systems involving polymers. The only studies we are aware of are those of Berry and Pritchet,[5] who studied the stresses induced by the diffusion of moisture in epoxy on copper cantilever beams, and of Tong and Saenger,[6] who studied the stress development during water transport in ultrathin polymethyl methacrylate (PMMA) films on quartz beams by the same method. In either case, the polymer picked up a relatively small amount of the penetrant without causing appreciable swelling. There seem to be no quantitative treatments of stress development during the transport of strong swelling agents in multilayered systems. In such systems, the polymer dimensional changes during transport and the accompanying stress effects may be very large.

In this article, we analyze the behavior of a bending beam during the absorption of a swelling agent by a thin polymer coating as a model for studying solvent-induced stress effects in multilayered systems. The bending beam provides the basis of a re-

* To whom correspondence should be addressed.

Journal of Applied Polymer Science, Vol. 43, 709–721 (1991)
© 1991 John Wiley & Sons, Inc. CCC 0021-8995/91/040709-13$04.00

liable, unambiguous experiment: One measures the deflection of the free end of a polymer-film-coated cantilever beam during solvent absorption using one laser pointer impinging upon the free end of the beam.[6] Stress is implied by the bending curvature obtainable from the end defection data.

With a suitable mechanical model, one can relate the bending curvature to the transport-induced stresses in the polymer film. In what follows, we develop such a model for the bending curvature of a polymer-coated beam using a phenomenological description of non-Fickian transport often encountered in glassy polymer/solvent systems. Based on this description, two limiting cases are studied to show the effects of polymer film thickness and solvent softening of the film. We then use the model to analyze the bending curvature data for the polyimide (PI)/quartz-*n*-methyl-2-pyrrolidone (NMP) system. The swelling process in a similar system was recently studied by Tong and coworkers[7] by an interferometric method. Using the present mechanical model, we show that the bending beam data can be predicted quantitatively from the earlier swelling data. This gives confidence that the stresses predicted by the model are quantitatively accurate.

BACKGROUND

It is helpful to review briefly the basis of transport of solvents in glassy polymers. One can think of two situations for unsteady penetrant transport in polymers according to the magnitude of the concentration interval for the process, i.e., according to the difference between initial and final penetrant concentrations. When the interval is relatively small, the material properties of the system remain practically constant and are well represented by average values. In this case, one can call the transport process linear because a mathematical representation would be a linear problem. When the concentration interval is large enough so that concentration-dependent material properties vary strongly as a function of time and position throughout the process, the transport can be called nonlinear.

For the linear case, Vrentas et al.[8] correlated the observed transport behavior with the value of the diffusion Deborah number $(DEB)_d$, defined as the ratio of a characteristic time for macromolecular relaxation to a characteristic time for diffusion. They suggested that the transport should be Fickian if the value of Deborah number is either very large or very small; non-Fickian effects should occur when Deborah number is $\sim \mathbf{O}(1)$. This notion has been generalized to the nonlinear case by Billovits and Durning,[9] who proposed that non-Fickian effects occur whenever the local $(DEB)_d$ passes through $\mathbf{O}(1)$. For both the linear and nonlinear cases, there is a modicum of experimental support for the Deborah number correlation. This indicates that the diffusion is coupled to macromolecular reconfiguration in the non-Fickian processes.

Alfrey and coworkers[10] first organized the non-Fickian behaviors observed for sorption when the concentration interval is large (i.e., for the nonlinear case). They found that all behaviors lie between two extreme limiting cases, Fickian and "Case II."

Case II has the following features[11,12]:

1. Concentration profiles with a sharp boundary separating the swollen region with equilibrium solvent content from a glassy region where the solvent concentration is negligible.
2. The sharp boundary moves through the polymer with a velocity that is constant in time.
3. A small "Fickian precursor" exists in the glassy region just ahead of the boundary.
4. There exists an induction time during which the sharp boundaries are set up.
5. There exists a tendency toward Fickian-like behavior (diffusion-controlled behavior) when the concentration gradient behind the boundary becomes significant.

There is now reasonable evidence that the non-Fickian transport of organic penetrants in glassy polymers is the result of a coupling between the diffusion of penetrant due to an activity gradient and the time-dependent response of the polymer "network" to diffusion-induced deformation (i.e., "swelling"). This notion is consistent with the Deborah number correlation. In Fickian diffusion, at one extreme the response of the polymer network to swelling is rapid so the penetrant diffusion controls the process. At the other extreme, Case II transport, the mechanical response of polymer to swelling controls the process. The dynamic response in this case is the development of a moving boundary. Many attempts have been made to model the nonlinear, non-Fickian diffusion. The works by Astarita and Sarti[12] and by Thomas and Windle[13] are the most successful. Billovits and Durning[11] concluded that these two models are conceptually similar and complementary. In this article, the transport of solvents in a polymer-coated beam is modeled after Astarita and Sarti (A–S). The reader can find thorough discussions of the A–S model in Ref.[12].

MODEL OF THE BENDING CURVATURE OF A POLYMER-COATED CANTILEVER BEAM DUE TO THE ABSORPTION OF SOLVENT

We use elementary beam theory[14] to analyze the flexure of a polymer-coated beam during the absorption of a penetrant by the coating. The analysis follows the line of thought of Berry and Pritchet.[5] Figure 1 shows a schematic of the coated cantilever beam. Initially, the coated beam has a curvature, R_i^{-1}, which indicates an initial equilibrated state of the stresses within the coating and the substrate. This initial stress state could result from, for example, the shrinkage of the coating due to drying during the preparation of the coated beam. The coated beam is suddenly immersed in an organic penetrant that diffuses into the coating, causing substantial swelling of the polymer layer perpendicular to the interface between polymer coating and substrate. The analysis for the absorption effect is relative to the initial state of the beam. We assume that:

1. Only one-dimensional transport of penetrant occurs (along z direction) and the A–S model accurately describes the transport. This implies that during the transport there exists a highly swollen layer of thickness λ and a nearly dry polymer layer of thickness δ, separated by a sharp moving boundary. The polymer (both swollen and unswollen portions) and the substrate of thickness h are Hookean elastic materials with constant moduli.
2. Plane cross-sections of the beam remain plane; this gives that all three shearing strains are zero, $\gamma_{xy} = \gamma_{xz} = \gamma_{yz} = 0$.
3. The cantilever beam acts like a composite narrow plate in which the normal strain in x direction, ϵ_{xx}, equals the normal strain in y direction, ϵ_{yy}, ($\epsilon_{xx} = \epsilon_{yy} \equiv \epsilon$); the same holds for the corresponding normal stresses, i.e., $\sigma_{xx} = \sigma_{yy} \equiv \sigma$.
4. The beam is traction free so that the net stress over the beam surface is zero; in particular, the normal stress in z direction, σ_z, is zero and shear stresses, τ_{xz} and τ_{yz}, are zero. This is a plane stress case.
5. The polymer thickness change caused by penetrant is much less than the lateral dimension of the polymer-coated beam.

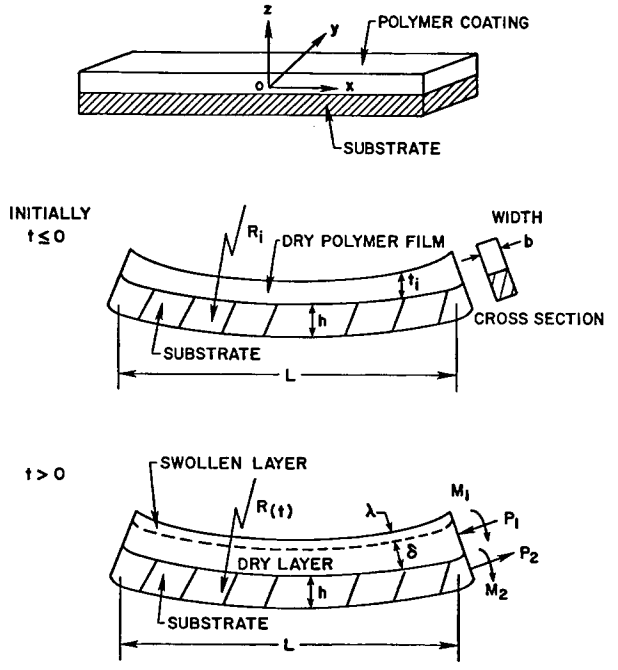

Figure 1 Schematic of a coated, cantilever beam during a swelling process.

From Hook's law, one obtains:

$$\sigma = [E/(1-\nu)]\epsilon \equiv E'\epsilon, \tag{1}$$

where E is the Young's modulus of a material, ν the Poisson's ratio of the material, and E' the elastic stiffness.

A "Trilayer" Model

Figure 1 shows all the relevant dimensions. The polymer film has width b, initial thickness t_i and length L. First, consider the polymer film alone, detached momentarily from a precurved beam and free from any external force as shown in Figure 2(a). The midplane of the detached film is $z = 0$, approximately the neutral axis. The subscripts s and g denote quantities referring to the swollen and dry layers, respectively. Applying eq. (1) gives:

$$\sigma/E' = \epsilon = \epsilon_{\text{abs}} - \epsilon_d - \epsilon_{\text{bend}}.$$

Here, ϵ_{abs} is the strain caused by local isotropic swelling:

$$\epsilon_{\text{abs}} = S*c(z,t),$$

where $c \equiv \rho_1/(\rho_2*\hat{v}_2)$ with ρ_1 being the density of penetrant, ρ_2 the density of polymer, $\hat{v}_2$ the partial specific volume of polymer, and t the time. If the excess volume is neglected, $S \equiv \hat{v}_1/3$ with $\hat{v}_1$ being the partial specific volume of the penetrant. Also, ϵ_d

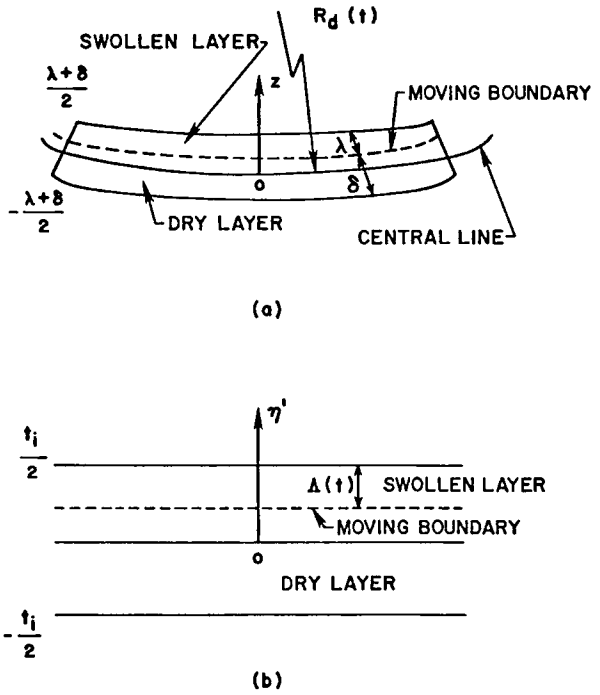

Figure 2 Schematic of (**a**) the detached polymer film and (**b**) the corresponding one-dimensional polymer material coordinates, η'.

is an unknown normal strain at the midplane determined by the force and moment balances on the cross-section of the detached layer and ϵ_{bend} is the strain relative to the midplane ($z = 0$) due to bending:

$$\epsilon_{\text{bend}} = z/R_d(t),$$

where $R_d(t)$ is the radius of curvature of the detached layer.

Substituting gives

$$\sigma(z, t)/E' = Sc(z, t) - \epsilon_d(t) - z/R_d(t). \quad (2)$$

Performing the usual normal force and moment balances on any cross-section of the detached layer gives the following expression for $R_d^{-1}(t)$:

$$1/R_d(t) = 24(m_2)S\langle cz\rangle/t_{\text{exp}} - 3(m_1)S\langle c\rangle/t_{\text{exp}}. \quad (3)$$

Here, the parameters m_1 and m_2 are defined as follows:

$$m_1 \equiv 8E'_sE^{(2)}/(8E^{(3)}E^{(1)} - 3(E^{(2)})^2) \quad (4)$$

$$m_2 \equiv 8E'_sE^{(1)}/(8E^{(3)}E^{(1)} - 3(E^{(2)})^2), \quad (5)$$

where the quantities $E^{(1)}$, $E^{(2)}$, and $E^{(3)}$ have the units of modulus (dynes/cm^2) and are given in Appendix A. The zero moment $\langle c\rangle$ and the first moment $\langle cz\rangle$ of the penetrant concentration c are defined and approximated as below to account for the swelling effect:

$$\frac{1}{t_{\text{exp}}}\int_{(\delta-\lambda)/2}^{(\lambda+\delta)/2} c(z, t)\,dz \approx \frac{1}{t_i}\int_{t_i/2-\Lambda(t)}^{t_i/2} c(\eta', t)\,d\eta' \equiv \langle c\rangle \quad (6)$$

$$\frac{1}{t_{\text{exp}}^2}\int_{(\delta-\lambda)/2}^{(\lambda+\delta)/2} zc(z, t)\,dz \approx \frac{1}{t_i^2}\int_{t_i/2-\Lambda(t)}^{t_i/2} c(\eta', t)\eta'\,d\eta' \equiv \langle cz\rangle, \quad (7)$$

where η' is the z-directed dimension in the polymer material coordinate[7] having the same origin as z [Fig. 2(b)], $\Lambda(t)$ the position of swollen-dry interface (moving boundary) in η', and $t_{\text{exp}}(= \lambda(t) + \delta(t))$ the measurable total polymer film thickness.

Note that eq. (3) gives correct limiting results: A flat detached layer results either without the absorption of penetrant or with a uniform distribution of penetrant; a flat layer also results if the modulus of the swollen portion is negligible ($E'_s/E'_g \ll 1$).

The analysis of the detached layer allows a simple calculation of the measurable coated beam curvature by "recombining" the detached polymer film and the substrate using suitable matching conditions. Let E'_p be an appropriate average of E'_s and E'_g. According to reference,[14] one can derive:

$$E'_p \equiv [E'_g/(t_{\text{exp}}^3)][\delta^3 + E'_s/E'_g(t_{\text{exp}}^3 - \delta^3)]$$

as the appropriate composite modulus used in the following development. Also, a force balance on the cross-section of the polymer-coated beam gives (see Fig. 1):

$$-P1 + P2 = 0, \quad \text{or } P1 = P2 = P,$$

where $P1$ is the net compressive normal force exerted on the polymer film by the substrate due to the adsorption of penetrant and $P2$ the net tensile normal force exerted on the substrate by the polymer layer due to the same cause.

Now, a moment balance on the cross-section of the coated beam gives one matching condition:

$$M_1 + M_2 - P(h + \lambda + \delta)/2 = 0, \quad (8)$$

where M_1 is the swelling-induced bending moment acting on the cross-section of the polymer layer, M_2 the swelling-induced bending moment on the cross-section of the quartz substrate (see Fig. 1), and $P(h + \lambda + \delta)/2$ the "resisting" moment. Since we assume the bending beam is linear elastic, the moment–curvature equation from elementary beam theory[14] gives

$$M_1 = E'_p I_p [1/R(t) - 1/R_d(t) - 1/R_i]$$
$$M_2 = E'_q I_q [1/R(t) - 1/R_i],$$

where $R^{-1}(t)$ is the measured bending curvature of the coated beam, I_p is the moment of inertia of the cross-section area of the polymer film, $I_p = bt_{\text{exp}}^3/12$, and I_q is that of the substrate, $I_q = bh^3/12$. Then, eq. (8) becomes:

$$1/2P(h + \delta + \lambda) = [1/R(t)](E'_p I_p + E'_q I_q) - E'_p I_p [1/R_d(t) + 1/R_i] - E'_q I_q / R_i.$$

A second mechanical matching condition is that the polymer normal strain matches the substrate strain at the film/substrate interface: $\epsilon_{\text{poly}} = \epsilon_q$. One has

$$\epsilon_{\text{poly}} = S\langle c \rangle - P/(E'_p t_{\text{exp}} b) - t_{\text{exp}}/2[1/R(t) - 1/R_i],$$

where $S\langle c \rangle$ gives the uniform expansion of polymer film due to $\langle c \rangle$. Also, $\epsilon_q = P/(E'_q hb) + h/2[1/R(t) - 1/R_i]$. Consequently,

$$S\langle c \rangle - P/(E'_p t_{\text{exp}} b) - t_{\text{exp}}/2[1/R(t) - 1/R_i] = P/(E'_q hb) + h/2[1/R(t) - 1/R_i].$$

Eliminating P from the two matching conditions leads to the following equation for the bending curvature of the polymer coated beam $1/R(t)$ as:

$$A(t)[1/R(t) - 1/R_i] = S\langle c \rangle + B(t)/R_d(t). \quad (9)$$

$A(t)$ and $B(t)$ both have units of length and are defined in Appendix A. Note that $B(t) < A(t)$.

At equilibrium, one has $c(t \to \infty) \equiv c_\infty$, a constant equilibrium concentration, $R(t \to \infty) \equiv R_\infty$, the equilibrium bending curvature, $A(t \to \infty) \equiv A_\infty$, and $R_d^{-1}(t \to \infty) = 0$. So, from eq. (9)

$$A_\infty(1/R_\infty - 1/R_i) = Sc_\infty, \quad (10)$$

which is the same as the equilibrium result of Berry and Prichet.[5]

Now, let us introduce a dimensionless form of eq. (9) with the following dimensionless quantities:

scaled bending curvature

$$\gamma \equiv [R^{-1} - R_i^{-1}]/(R_\infty^{-1} - R_i^{-1})$$

dimensionless initial film thickness

$$a_1 \equiv t_i/h$$

swelling film thickness ratio

$$\theta \equiv (t_{\text{exp}} - t_i)/t_i$$

dimensionless moduli ratio

$$k_1 \equiv E'_p/E'_q = [E'_g/(E'_q t_{\text{exp}}^3)][\delta^3 + E'_s/E'_g(t_{\text{exp}}^3 - \delta^3)] = [E'_g/(E'_q t_{\text{exp}}^3)][\delta^3 + k_2(t_{\text{exp}}^3 - \delta^3)].$$

One can rewrite the expressions for $A(t)$ and $B(t)$ in terms of these dimensionless quantities as shown in Appendix A. With these dimensionless quantities, the dimensionless bending curvature γ is given by

$$\gamma = q_1 Z + q_2 F, \quad (11)$$

where eq. (3) for $R_d(t)$ has been used. The dimensionless quantities q_1 and q_2 are

$$q_1 \equiv \frac{A_\infty}{A} - \frac{3m_1 A_\infty B}{ASha_1(1 + \theta)} \quad (12)$$

$$q_2 \equiv \frac{24m_2 A_\infty B}{Aha_1(1 + \theta)} \quad (13)$$

These depend both on the transport and mechanical properties of the system. The dimensionless moments in eq. (11), Z and F, are

$$Z \equiv \frac{\langle c \rangle}{c_\infty} \quad (14)$$

$$F \equiv \frac{\langle cz \rangle}{c_\infty}. \quad (15)$$

Equation (11) allows the calculation of bending curvature of a beam system with any concentration profile possessing a sharp moving boundary, provided that the mechanical properties of the system are known. In the absence of the moving boundary, one can still use eq. (11) by simply eliminating the dry layer in Figure 1, i.e., setting $\delta = 0$. Equation (11) properly satisfies the two limits: at $t = 0$, $\gamma = 0$ and at $t \to \infty$, $\gamma = 1$.

A Useful Simplification

In the above discussion, we have included the feature that the swollen and dry layers have significantly different moduli. This is usually observed when Case II diffusion takes place. It can occur, however, that there is virtually no change in the moduli upon swelling, in which case we can simplify the results of the previous section. Since in this case, $E'_s = E'_g$, i.e., $k_2 = 1$, the average Young's modulus of the polymer film E'_p is $E'_p = E'_s = E'_g$. This simplifies the quantities q_1 and q_2 to:

$$q_1 = \frac{A_\infty}{A} \tag{16}$$

$$q_2 = \frac{12A_\infty B}{Aha_1(1+\theta)}. \tag{17}$$

Time-dependent Concentration Profile and Film Thickness

The calculation of the bending curvature requires the concentration distribution, $c(\eta', t)$, the measurable film thickness, t_{exp}, and the thicknesses of the swollen (λ) and dry (δ) layers.

A schematic representation of the one-dimensional penetrant concentration profile in the NMP–PI system inferred from an earlier study[7] is given in Figure 3. Here the polymer material coordinate η (note that η is different from η', $\eta = t_i/2 - \eta'$) is related to the lab coordinate z by

$$\partial\eta/\partial z = \rho_2\hat{v}_2. \tag{18}$$

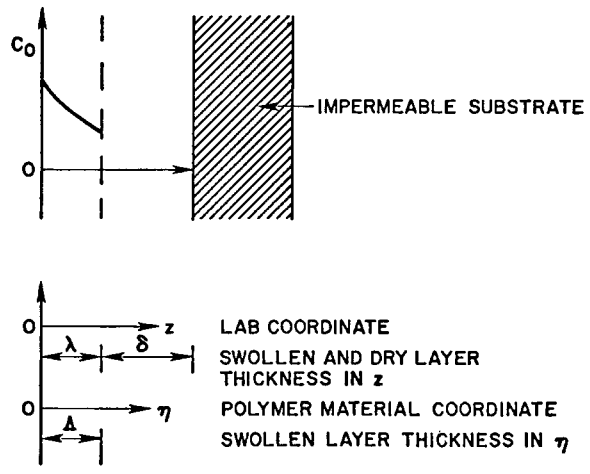

Figure 3 Schematic of penetrant concentration profile, the lab (z) and polymer material (η) coordinates.

From eq. (18):

$$t_{exp} = \int_0^{t_i} \frac{1}{\rho_2\hat{v}_2}\,d\eta = t_i + \hat{v}_1\int_0^{t_i} c(\eta, t)\,d\eta. \tag{19}$$

Note that at equilibrium

$$t_{exp} = t_{eq} = t_i + \hat{v}_1 c_\infty t_i = (t_i/(\rho_2\hat{v}_2))_\infty.$$

Now, to evaluate q_1 and q_2 in eq. (11), the expressions of $\delta(t)$ and $\lambda(t)$ are needed. From eq. (18), we have:

$$\lambda(t) = \Lambda(t) + \hat{v}_1\int_0^{\Lambda(t)} c(\eta, t)\,d\eta \tag{20}$$

and since $\delta(t)$ is the thickness of dry layer we have:

$$\delta(t) = t_i - \Lambda(t). \tag{21}$$

Now, the A–S model[12] supplies simple formulae for $c(\eta, t)$ and $t_{exp}(t)$ in the polymer material coordinate, η, for three cases:

1. A diffusion-controlled moving boundary process (Fickian-like).
2. The Case II diffusion.
3. An "intermediate" case between (a) and (b).

Appendix B gives the dimensional form of these formulae, as well as expressions for $\delta(t)$ and $\lambda(t)$ for each of the three cases.

GENERIC STUDY OF BENDING BEHAVIOR DURING THE TWO LIMITING CASES: CASE II AND DIFFUSION-CONTROLLED TRANSPORT

To see the characteristic bending behavior of a polymer film coated beam due to the absorption of a penetrant, we calculate the bending curvature for two limiting transport cases: Case II and diffusion controlled. The calculations illustrate that the bending beam can offer a method of detecting the transport mechanism in the deposited film. To be definite, we employ mechanical and transport properties on the order of those for the PI/quartz-NMP system studied recently by interferometry. We study how γ is affected by the relative thicknesses of the polymer film and quartz substrate (a_1), and the relative moduli of the swollen and glassy layers of the polymer (k_2). The other necessary properties of the beam system are summarized in Table I.

Table I Properties Needed for the Preparation of Figures 4 and 5

Property	Value
Thickness of substrate	$h = 0.01$ cm
Thickness of initial polymer film	$t_i = 5 \times 10^{-4}$ cm
Partial specific volume of solvent	$\hat{v}_1 = 1.0$ cm^3/g
Equilibrium solvent concentration	$c_\infty = 0.2$ (g solvent/cm^3 polymer)
Young's modulus of polymer film	$E_g = 10^{10}$ dynes/cm^2
Young's modulus of substrate	$E_q = 10^{12}$ dynes/cm^2
Poisson's ratio of polymer film	$\nu_g = 0.45$
Poisson's ratio of substrate	$\nu_q = 0.15$
Equilibrium thickness swelling ratio	$\theta_\infty = 0.17$

Equation (11) is used to calculate the dimensionless curvature γ. Computer programs were developed to evaluate the quantities q_1 [eq. (12)], q_2 [eq. (13)], Z [eq. (14)], and F [eq. (15)] employing necessary properties from Table I and appropriate equations in Appendix B for the two different transports. Results are shown in Figures 4–7.

Figures 4 and 5 show both the swelling ratio θ and the dimensionless curvature γ for Case II plotted against scaled time $\tau \equiv tv_o/t_i$, where v_o is the velocity of the moving boundary. Figure 4 shows the effect on γ of the ratio $a_1 = t_i/h$ when the swollen and dry layers have the same modulus, $k_2 = 1.0$, i.e., assuming no solvent softening effect. It is clear that the thickness ratio affects the bending curvature, γ, significantly. As the value of a_1 is increased through 0.1, the γ curve becomes concave down. In the usual case, where the coating is much thinner than the substrate, the bending curvature is linear with time, in parallel with the swelling ratio θ. Figure 5 shows the effect on γ of the modulus ratio k_2 with $a_1 = 0.1$ to examine the solvent softening effect. It is found that a difference between the moduli of the swollen and dry layers does not much affect the bending behavior when the coating is much thinner than the substrate. As the solvent softening effect becomes more significant, i.e., as the value of k_2 decreases from 1.0 to 0.01, the γ curves almost overlap and are all linear with time. Typically, the swollen layer is softened by swelling ($k_2 < 1$) in real systems; therefore, one expects that both θ and γ should show linear increases in time for thin deposited films ($a_1 \leq 0.1$) during the case II transport.

For the diffusion-controlled case, one sees similar effects of a_1 and k_2. Figures 6 and 7 show both the θ and γ for the diffusion-controlled case plotted against the square root of dimensionless time, $\sqrt{\tau} \equiv \sqrt{(Dt/t_i^2)}$, where D is an effective diffusion coefficient in the polymer material coordinate. Figure 6 shows the effect of a_1 on γ with $k_2 = 1.0$. For thin coatings ($a_1 \leq 0.1$), the γ and θ curves are both linear with $\sqrt{\tau}$. It is found that increasing a_1(a_1

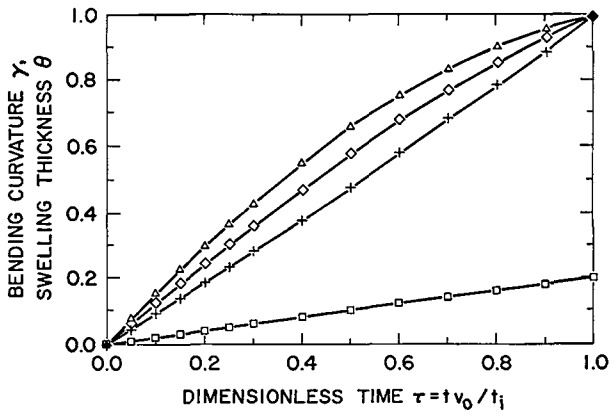

Figure 4 Swelling ratio, $\theta(\square)$, and bending curvature, γ, vs. $\tau = v_o t/t_i$ for the Case II diffusion. The parameters are as in Table I with $k_2 = 1.0$ and for several values of a_1[0.1(+), 1($\diamond$), 2.0($\triangle$)].

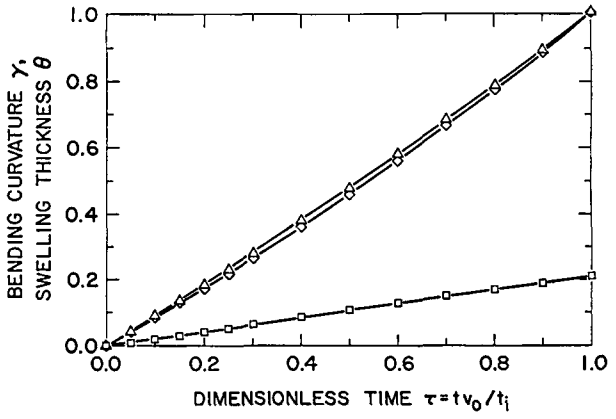

Figure 5 Swelling ratio, $\theta(\square)$, and bending curvature, γ, vs. $\tau = v_o t/t_i$ for the Case II diffusion. The parameters are as in Table I with $a_1 = 0.1$ and for several values of k_2[0.01(+), 0.1($\diamond$), 1.0($\triangle$)].

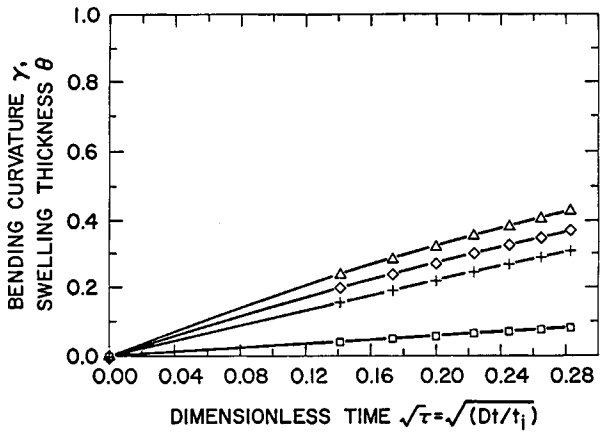

Figure 6 Swelling ratio, $\theta(\square)$, and bending curvature, γ, vs. $\sqrt{\tau} = \sqrt{(Dt/t_i)}$ for the diffusion-controlled transport. The parameters are as in Table I with $k_2 = 1.0$ and for several values of a_1[0.1(+), 1(◇), 2.0(△)].

> 0.1) causes the γ curve to become concave down, deviating from the swelling behavior, reminiscent of the behavior during case II (see Fig. 4). Also, the higher the value of a_1, the higher the initial bending rate. Figure 7 shows the effect on γ of k_2 for a thin film ($a_1 = 0.1$). One can see that the γ curves for various k_2 (0.01, 0.1, 1.0) are linear with $\sqrt{\tau}$ and almost overlap. Clearly, in a real system one can expect that both θ and γ increase linearly with $\sqrt{\tau}$ for thin deposited films during diffusion-controlled transport.

In summary, from the above study it is most interesting to find that when the polymer film is much thinner ($a_1 \leq 0.1$) than the substrate the solvent softening effect does not influence the bending behavior and the bending parallels the film swelling. These results suggest that the bending beam can be used as a direct method to study the transport mechanism of solvents in supported glassy polymer films, provided the initial film thickness is significantly less than the substrate thickness.

EXPERIMENTAL

The bending beam experiment performed in this study is identical to that reported recently for the study of water transport in PMMA.[6] In our bending beam experiment, one spincasts the polymer film of interest on one side of a slender, rigid beam such as fused quartz. One end of the coated beam is then clamped (vertically) with the unclamped length being ~3 cm. A low-power laser (~ 1 mW He-Ne laser at 6328 Å) is then directed onto the free end of the beam and the position of the reflected ray is marked on a vertically mounted paper about 1 m away. Then, the beam is exposed to the liquid penetrant, which diffuses into the polymer coating, inducing curvature that changes with time. The induced curvature shifts the reflected ray's position until sorption equilibrium is reached. From the reflected ray's position and simple geometric considerations, the beam curvature (R^{-1}) can be calculated as a function of time until the absorption equilibrium is reached.

Thin fused quartz beams (3.8 cm long, 0.3 cm wide, and ~0.0076 cm thick) were coated by curing the spun-on PI precursor, polyamic acid in NMP, to 400°C in nitrogen. NMP for the bending beam experiment (from Aldrich, HPLC grade) was used as received. For each bending beam experiment, the dry PI thickness (~ 5 μm) was determined by the weight, density, and lateral dimensions of the beam and checked with a stylus profilometer. The experiments were performed at room temperature (20°C) and 80°C.

RESULTS AND DISCUSSION

Analysis of the Experimental Bending Curvature Data

In the earlier study of Tong et al.,[7] the formulae for the three cases of the A–S model discussed earlier were fit to θ vs. t data determined by interferometry. The analysis showed that the "intermediate" case gave the best representation of the data. The parameters for the NMP sorption experiments at 20

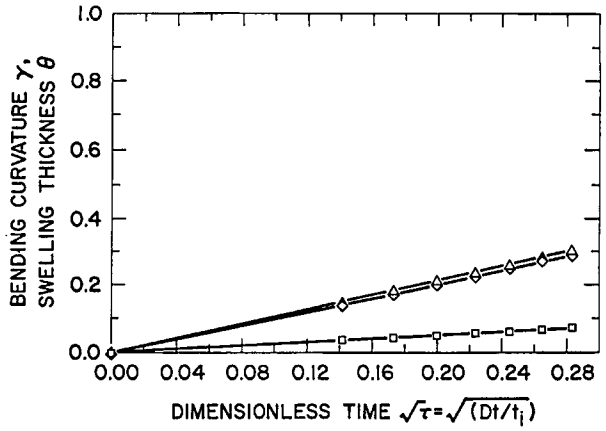

Figure 7 Swelling ratio, $\theta(\square)$, and bending curvature, γ, vs. $\sqrt{\tau} = \sqrt{(Dt/t_i)}$ for the diffusion-controlled transport. The parameters are as in Table I with $a_1 = 0.1$ and for several values of k_2[0.01(+), 0.1(◇), 1.0(△)].

Table II Summary of the Transport Parameters From Interferometry[7]

No.	Case	Effective Diffusivity ($cm^2/sec, \times 10^{12}$) 20°C	Effective Diffusivity ($cm^2/sec, \times 10^{12}$) 80°C	Boundary Velocity ($cm/sec, \times 10^{9}$) 20°C	Boundary Velocity ($cm/sec, \times 10^{9}$) 80°C
1	Diffusion-controlled case	0.85	66		
2	Intermediate process	2.8	100	6.0	175
3	Case II transport			4.4	460

and 80°C extracted from the least-square fits are summarized in Table II. The prediction of γ for the three cases, namely, diffusion controlled, case II, and "intermediate" transport, were done by using eq. (11), the pertinent formulae in Appendix B with transport parameters in Table II, and the auxiliary physical data in Table III. Because the difference in moduli of the swollen and dry PI film was found to be negligible,[3] we set $k_2 = 1$, and use the simplified formulas [eqs. (16) and (17)] for the calculations of q_1 and q_2 in eq. (11). The results are plotted in Figures 8 (20°C) and 9 (80°C) against the scaled time, $\tau = D_{exp}t/t_i^2$, together with the experimental bending curvature data. The diffusion coefficient D_{exp} is that from Table II for the intermediate transport at 20 and 80°C, respectively. Clearly, the predictions of the intermediate case give the best matches to the data at both temperatures. In fact, the quantitative agreement is reasonably good. Note also that for our beam system the thickness ratio is small, $a_1 = 0.0656$ (<0.1), and that the experimental data appear to parallel the swelling behavior. This is exactly the behavior predicted in the previous section for the Case II and diffusion-controlled transport. In summary, the calculations encourage that our simple mechanical model can predict the bending behavior of a coated beam well enough for engineering purposes.

Estimation of the Swelling-Induced Stress

As mentioned in the introduction, the stress development induced by the absorption of a swelling agent in a supported polymer thin film is not yet well understood. It is thought that during some circuit board processes solvent transport can induce residual stresses approximately equal to those due to temperature changes alone. To check this, we evaluated the swelling-induced stresses to compare them with the stresses due to thermal "curing" alone.

The mean normal stress in the polymer coating, induced by the absorption of a penetrant, can be estimated by dividing the compressive normal force P_1 ($= P$) by the cross-sectional area of the coating $t_{exp}b$ and denoted by $\Delta\sigma_m$, indicating the stress change relative to the initial stress state.

$$\Delta\sigma_m = P/(t_{exp}b). \tag{22}$$

Table III Mechanical and Geometric Constants for the Bending Beam

Constant	20°C	80°C
Thickness of quartz substrate, h (cm)	7.62×10^{-3}	same
Thickness of initial polymer film, t_i (cm)	5×10^{-4}	same
Beam length, l (cm)	3	2.7
Partial specific volume of NMP, $\hat{v}_1$ (cm^3/g)[15]	1.027	same
Equilibrium NMP concentration, c_∞ (g NMP/cm^3 PI)	0.2	same
Young's modulus of glassy PI film, E_g ($dynes/cm^2$)[3]	1.4×10^{10}	same
Young's modulus of quartz beam, E_q ($dynes/cm^2$)[16]	7.3×10^{11}	same
Poisson's ratio of glassy PI film, ν_g[17]	0.45	same
Poisson's ratio of quartz substrate, ν_q[16]	0.16	same
Equilibrium thickness swelling ratio, θ_∞[7]	0.17	same
Equilibrium bending curvature, R_∞^{-1}	0.004	0.0005
Initial bending curvature, R_i^{-1}	0.02836	0.02608

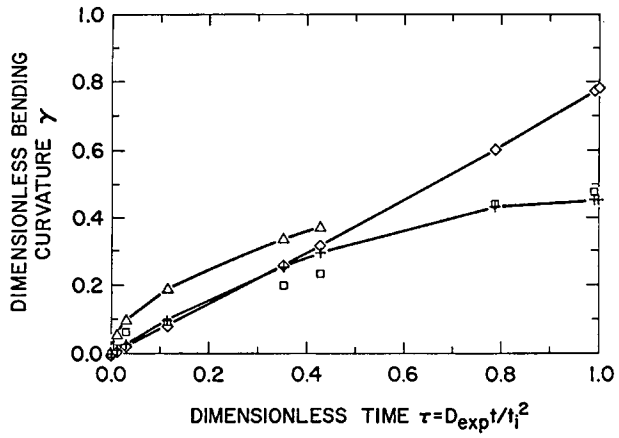

Figure 8 Comparison of the predicted curvature γ for the three cases (Δ, diffusion controlled; +, intermediate; $\diamond$, Case II) with the experimental bending curvature ($\square$) (at 20°C). The corresponding values of the model parameters are given in Tables II and III.

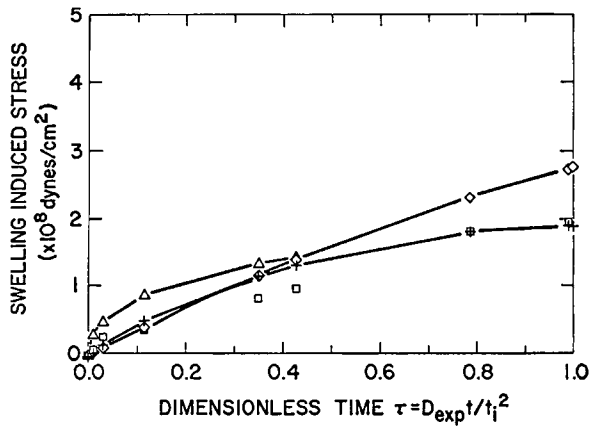

Figure 10 Comparison of the estimated swelling-induced stress, $\Delta\sigma_m$, for the three cases (Δ, diffusion controlled; +, intermediate, $\diamond$, Case II) with that, $\Delta\sigma_{exp}$($\square$), from the initial film thickness t_i and the experimental curvature (at 20°C).

From eqs. (8) and (3) with assuming $E'_s = E'_g$, one can get

$$\Delta\sigma_m = \{1/[6t_{exp}(h + t_{exp})]\}\{(E'_p t_{exp}^3 + E'_q h^3) \times (R^{-1} - R_i^{-1}) - 12Sc_\infty E'_p t_{exp}^2 F\}$$

or in terms of dimensionless quantities

$$\Delta\sigma_m = \frac{1}{6a_1h^2(\theta+1)[a_1(\theta+1)+1]} \times \{E'_q h^3[k_1 a_1^3(\theta+1)^3 + 1](R_\infty^{-1} - R_i^{-1})\gamma - 12Sc_\infty k_1 a_1^2 E'_q h^2(\theta+1)^2 F\}. \quad (23)$$

When the coating is significantly thinner and softer than the substrate, i.e., $a_1 \ll 1$ and $k_1 \ll 1$, then eq. (23) can be simplified to

$$\Delta\sigma_m = \frac{E'_q h^2 (R^{-1} - R_i^{-1})}{6t_{exp}}. \quad (24)$$

Equation (24) gives the same stress-bending curvature relation used in Refs. 1–3, 17, and 18 for the study of stress development during heat treatments using originally flat coated beams ($R_i^{-1} = 0$).

We used two procedures to estimate the swelling-induced stress from eqs. (23) and (24). In the first, it was calculated using eq. (24) assuming $t_{exp} \approx t_i$ and using experimental curvature data; this value is denoted by $\Delta\sigma_{exp}$. In the second, we used eq. (23)

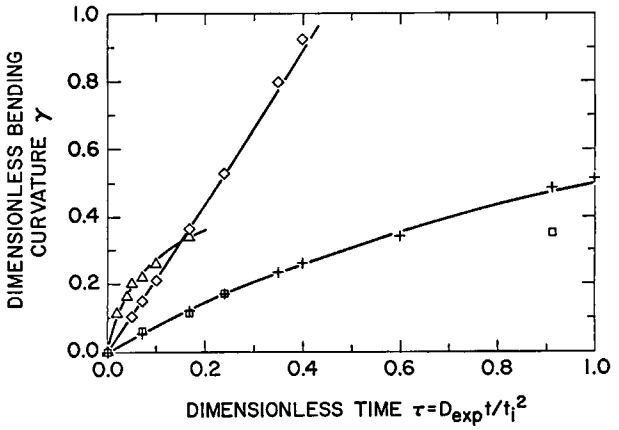

Figure 9 Comparison of the predicted curvature γ for the three cases (Δ, diffusion controlled; +, intermediate; $\diamond$, Case II) with the experimental bending curvature ($\square$) (at 80°C). The relevant values of the model parameters are given in Tables II and III.

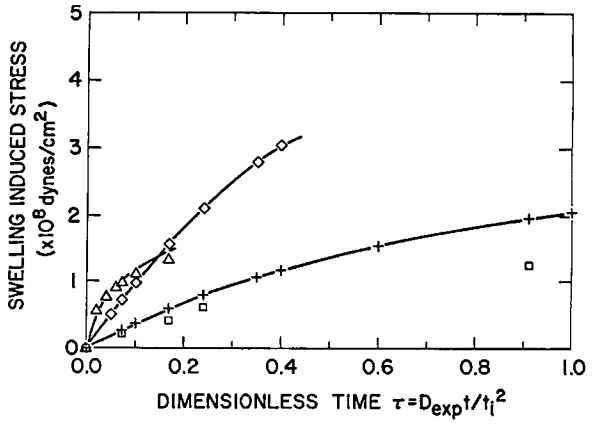

Figure 11 Comparison of the estimated swelling-induced stress, $\Delta\sigma_m$, for the three cases (Δ, diffusion controlled; +, intermediate.; $\diamond$, Case II) with that, $\Delta\sigma_{exp}$($\square$), from the initial film thickness t_i and the experimental curvature (at 80°C).

and the information for γ and θ from the previous section and the appropriate values of E_q', t_i, R_∞^{-1}, and R_i^{-1} from Table II; in this way, one can predict the stress for the three cases discussed earlier. All results are plotted in Figures 10 and 11 for 20 and 80°C, respectively. Note that our estimated residual stress ($< 2 \times 10^8$ dynes/cm^2) is on the same order as those previously reported[1,17] ($1–6 \times 10^8$ dynes/cm^2) for thermally induced stresses. The stress level is less than the yield strength of typical commercial PI films[19] (6.3×10^8 dynes/cm^2, at 3% yield strain), and far below its ultimate tensile strength (1.58×10^9 dynes/cm^2) at 298 K. This indicates that the PI film probably would not undergo plastic deformation or fracture.

CONCLUSIONS

We developed an elementary model for the calculation of the bending curvature of a polymer-film-coated beam induced by the non-Fickian adsorption of a low molecular weight species. It can be readily proved that, under proper simplification, the results of Berry and Pritchet[5] are recovered from the model (the Fickian case).

We showed the effects of both the polymer film thickness and solvent softening on the bending behavior. In general, when the deposited film is much thinner than the substrate ($a_1 \leq 0.1$), the bending kinetics parallel the swelling kinetics. This feature shows that the bending beam can provide the same information as a sorption experiment under these circumstances. Exactly this behavior is observed experimentally in our study of the NMP–PI system. The experimental analysis indicates that the bending induced by NMP sorption into the glassy PI film coated onto a quartz beam is indeed best described when using the "intermediate" transport model according to Astarita and Sarti; this is consistent with the conclusions of our recent laser interferometry study[7] of the swelling process. The estimation of the swelling-induced stress using the model shows that it is as important as that induced in the thermal "curing" process.

In summary, the work encourages that the simple mechanical model presented here accurately predicts swelling-induced stresses in thin deposited polymer films. This finding makes the model a useful tool for engineering calculations.

C. J. Durning and T. Z. Fu acknowledge partial financial support from the National Science Foundation (Grant CBT-86-17369). The authors thank Dr. B. J. Han for useful discussions.

NOMENCLATURE

b	beam width
c	local penetrant concentration ($\rho_1/\rho_2\hat{v}_2$)
c_∞	equilibrium penetrant concentration
c^*	threshold penetrant concentration
$\langle c \rangle$	first moment of penetrant concentration
$\langle cz \rangle$	second moment of penetrant concentration
D	diffusion coefficient in polymer material coordinate
E_j	Young's modulus of j; s, swollen polymer; g, glassy polymer; q, quartz
h	substrate thickness
L	beam length
I_j	moment of inertia of material layer j
M_1	bending moment on cross-section of polymer film
M_2	bending moment on cross-section of substrate
$R(t)$	radius of curvature of polymer-coated beam
P_1	net compressive normal force exerted on cross-section of polymer film by the substrate
P_2	net tensile normal force exerted on cross-section of the substrate by polymer film
$R_d(t)$	radius of curvature of detached polymer layer
R_∞	equilibrium radius of curvature of polymer-coated beam
S	swelling parameter ($\hat{v}_1/3$)
t	lab time
t_{exp}	experimental polymer film thickness in lab frame
t_i	initial film thickness
v	Poisson's ratio
$\hat{v}_i$	partial specific volume of component i; 1, penetrant; 2, polymer
v_o	initial velocity of moving boundary
z	distance in lab frame

Greek

θ	dimensionless polymer film thickness
ϵ_{abs}	local normal strain due to absorption of penetrant
η'	distance in polymer material coordinate (see Fig. 2(b))
η	distance in polymer material coordinate (see Fig. 3)
$\Lambda t)$	swollen layer thickness in the polymer material coordinate
γ_{ij}, $i \neq j$	shearing strain, $i = x, y, z$; $j = x, y, z$
σ_i	normal stress in direction i, $i = x, y, z$

ϵ_{ii} normal strain in direction i, $i = x, y, z$
ρ_i density of component i
ϵ_d normal strain at $z = 0$, the midplane (see Fig. 2(a))
ϵ_{bend} normal strain due to bending relative to $z = 0$
$\lambda(t)$ thickness of swollen layer in lab frame
$\delta(t)$ thickness of dry layer in lab frame
γ dimensionless bending curvature of bending beam

REFERENCES

1. B. J. Han, C. Gryte, H. M. Tong, and C. Feger, SPE Preprint, *ANTEC'88*, 994 (1988).
2. H. M. Tong, C. K. Hu, C. Feger, and P. S. Ho, *Polym. Eng. Sci.*, **26**(17), 1213 (1986).
3. Y. H. Jeng, IBM Res. Div., Almaden Research Center, private communication.
4. C. L. Bauer and R. J. Farris, "Polymers For High Technology, Electronics And Photonics," M. J. Bowden and S. R. Turner, Eds., *ACS Symposium Series 346*, 1986, Chap. 23, Americal Chemical Society, Washington DC, 1987.
5. B. S. Berry and W. C. Pritchet, *IBM J. Res. Dev.*, **28**(6), 662 (1984).
6. H. M. Tong and K. L. Saenger, *J. Appl. Polym. Sci.*, in press.
7. H. M. Tong, K. L. Saenger, and C. J. Durning, *J. Polym. Sci., Polym. Phys. Ed.*, **27**, 689 (1989).
8. J. S. Vrentas, C. M. Jarzebski, and J. L. Duda, *AICHE J.*, **21**, 894 (1975).
9. G. Billovits and C. J. Durning, *Chem. Eng. Commun.*, **82**, 21 (1989).
10. T. Alfrey, E. F. Gurnee, and W. G. Lloyd, *J. Polym. Sci.*, **C12**, 249 (1966).
11. G. F. Billovits and C. J. Durning, *Polymer*, **29**, 1468 (1988).
12. G. Astarita and G. C. Sarti, *Polym. Eng. Sci.*, **18**, 388 (1978).
13. N. L. Thomas and A. H. Windle, *Polymer*, **23**, 529 (1982).
14. R. Nelson and J. Bauld, *Mechanics of Materials*, Brooks/Cole Engineering Division, Monterey, 1982.
15. M-PYROL, N-methyl-2-pyrrolidone, GAF Corp., New York, 1972.
16. *American Institute of Physics Handbook*, 3rd ed., McGraw-Hill, New York, 1972.
17. B. J. Han, H. M. Tong, K. L. Saenger, and C. C. Gryte, *Mater. Res. Soc. Symp. Proc.*, **76**, 123 (1987).
18. D. S. Campbell, In *Handbook of Thin Film Technology*, L. I. Maisseland and R. Glang, Eds., McGraw-Hill, New York, 1970, Chap. 12.
19. M. I. Bessonov, M. M. Koton, V. V. Kudryavtsev, and L. A. Laius, *Polyimides—Thermally Stable Polymers*, Plenum, New York, 1987.

Received October 26, 1989
Accepted November 30, 1990

APPENDIX A

The quantities $E^{(1)}$, $E^{(2)}$, and $E^{(3)}$ in eqs. (4) and (5) are defined as follows:

$$E^{(1)} \equiv (1/t_{exp})[E'_g\delta(t) + E'_s\lambda(t)] \quad \text{(A1)}$$

$$E^{(2)}t_{exp}^2 \equiv [E'_g((\delta - \lambda)^2 - (t_{exp})^2) + E'_s((t_{exp})^2 - (\delta - \lambda)^2)] \quad \text{(A2)}$$

$$E^{(3)}t_{exp}^3 \equiv E'_g[(\delta - \lambda)^3 + t_{exp}^3] + E'_s[t_{exp}^3 - (\delta - \lambda)^3]. \quad \text{(A3)}$$

The quantities $A(t)$ and $B(t)$ in eq. (9) are:

$$A(t) \equiv \{1/[6(h + t_{exp})]\}(E'_pt_{exp}^3 + E'_qh^3) \times \{1/(E'_pt_{exp}) + 1/(E'_qh)\} + (h + t_{exp})/2 \quad \text{(A4)}$$

$$B(t) \equiv [2E'_pI_p/(h + t_{exp})] \times \{1/(E'_pt_{exp}b) + 1/(E'_qhb)\} = \{E'_pt_{exp}^3/[6(h + t_{exp})]\} \times \{1/(E'_pt_{exp}) + 1/(E'_qh)\}. \quad \text{(A5)}$$

All symbols are defined in the nomenclature.

A and B can be recast in terms of dimensionless quantities as:

$$A = \frac{h}{2}\left\{\frac{k_1a_1^3(1+\theta)^3 + 1}{3[1 + a_1(1+\theta)]}\left[\frac{1}{k_1a_1(1+\theta)} + 1\right] + 1 + a_1(1+\theta)\right\}$$

$$B = \frac{a_1^2(1+\theta)^2h}{6[1 + a_1(1+\theta)]}[1 + k_1a_1(1+\theta)].$$

APPENDIX B

Analytical penetrant concentration distributions for the three cases can be obtained from the A–S model. They are summarized below, along with the corresponding expression of the film thickness, t_{exp}, the swollen layer thickness (λ), and the dry layer thickness (δ).

DIFFUSION-CONTROLLED PROCESS

For the diffusion-controlled process, diffusion of the solvent in the swollen layer controls the moving boundary motion and the transport is Fickian-like. Referring to the discussion in Refs. 7 and 11, and assuming $t_i * v_0/D \gg 1$, where v_o is the moving boundary velocity, then

$$\Lambda = 2m\sqrt{Dt} \tag{B1}$$

and

$$c = c_\infty - (c_\infty - c^*) \times \{erf[\eta/(2\sqrt{Dt})]/erf(m)\}. \tag{B2}$$

Here, c^* is the threshold penetrant concentration defined in Ref. 11 and parameter m is the solution of

$$\sqrt{\pi * m * erf(m) * \exp(m^2)} = 1/q - 1.$$

where $q \equiv C^*/C_\infty$.

These are valid provided the moving boundary has not yet reached the substrate, i.e., $t < t_i**2/(4Dm^2)$. Substituting (B2) into eq. (19) and integrating gives:

$$t_{exp} = t_i + (2\sqrt{Dt})\hat{v}_1(c_\infty - c^*)/[\sqrt{\pi}erf(m)] \tag{B3}$$

or, for $c^*/c_\infty \ll 1$, which is usually found in glassy polymers/strong swelling agent pairs,[11,12]

$$t_{exp} \approx t_i + (2\sqrt{Dt})\hat{v}_1 c_\infty/[\sqrt{\pi}\,\mathrm{erf}(m)]. \tag{B4}$$

This shows, for the diffusion-controlled limit of Astarita and Sarti, that t_{exp} is proportional to $\sqrt{t}$.

The equations for $\lambda(t)$ and $\delta(t)$ can be derived readily from eqs. (20) and (21) as:

$$\delta(t) = t_i - \Lambda(t) = t_i - 2m\sqrt{Dt} \tag{B5}$$

$$\lambda(t) = 2\sqrt{Dt}(\hat{v}_1 c_\infty/(\sqrt{\pi}erf(m)) + m). \tag{B6}$$

It is apparent that the swollen region increases proportionally with $\sqrt{t}$ and the dry layer shrinks linearly with $\sqrt{t}$.

CASE II

For Case II limit, there is no penetrant diffusion limitation, and the moving boundary motion is controlled completely by the polymer deformation kinetics at the boundary. When $t_i v_o/D \ll 1$ and $t < t_i/v_o$,

$$\Lambda(t) = v_o t$$

and

$$c = c^* + (c_\infty - c^*)H[\Lambda(t) - \eta],$$

where H is the step function.

For $c^*/c_o \ll 1$,

$$c = c_\infty H[\Lambda(t) - \eta]. \tag{B7}$$

Substituting eq. (B7) into eq. (19) and integrating gives:

$$t_{exp} \approx t_i + \hat{v}_1 c_\infty v_o t. \tag{B8}$$

The linear time dependence of t_{exp} emerges from equation (B8), as expected.

The relations for $\delta(t)$ and $\lambda(t)$ are

$$\delta(t) = t_i - v_o t \tag{B9}$$

and

$$\lambda(t) = v_o(\hat{v}_1 c_\infty + 1)t. \tag{B10}$$

The swollen region grows linearly with time; at the same time, the dry layer contracts linearly with time.

INTERMEDIATE CASE

This behavior is realized when diffusion in the swollen region just begins to affect the boundary propagation for times when the film has not yet been completely penetrated: $t_i v_o/D < 1$ and $t < t_i/v_o$. A regular perturbation from case II transport yields:

$$\Lambda(t) \approx tv_o - nt^2 v_o**3/(2D)$$

and for $c^*/c_\infty \ll 1$,

$$c = c_\infty[1 - (\eta v_o/D) \times (1 - (1 + n)tv_o**2/D)]. \tag{B11}$$

where n is defined in Ref. 7.

Substituting eq. (B11) into eq. (19) and integrating gives:

$$t_{exp} \approx t_i + \hat{v}_1 c_o v_o t - \hat{v}_1 c_o(1 + n)v_o**3(t^2)/(2D). \tag{B12}$$

Similarly, $\delta(t)$ and $\lambda(t)$ are calculated by:

$$\delta(t) = t_i - v_o t + 1/2nv_o^3 t^2/D \tag{B13}$$

$$\lambda(t) = v_o(\hat{v}_1 c_\infty + 1)t - 1/2v_o^3 t^2/D(\hat{v}_1 c_\infty(1 + n) + n). \tag{B14}$$

Analogous to eq. (B12), $\lambda(t)$ is found to be a function of time raised to some power between 1/2 and 1.